Desalination and Water Treatment
www.deswater.com

doi: 10.1080/19443994.2015.1054315

57 (2016) 12822–12831
June

Taylor & Francis
Taylor & Francis Group

Adsorption of malachite green and crystal violet cationic dyes from aqueous solution using pumice stone as a low-cost adsorbent: kinetic, equilibrium, and thermodynamic studies

Hadi Shayesteh[a], Ahmad Rahbar-Kelishami[a,*], Reza Norouzbeigi[a,b]

[a]*Faculty of Chemical Engineering, Iran University of Science & Technology (IUST), Narmak, Tehran, Iran, Tel. +98 21 77451505; Fax: +98 21 77240495; emails: hadi_shayesteh@chemeng.iust.ac.ir (H. Shayesteh), ahmadrahbar@iust.ac.ir (A. Rahbar-Kelishami), norouzbeigi@iust.ac.ir (R. Norouzbeigi)*
[b]*Cement Research Center, Iran University of Science & Technology (IUST), Narmak, Tehran, Iran*

Received 28 February 2015; Accepted 15 May 2015

ABSTRACT

In this study, the sorption potential of pumice was investigated as geomaterial adsorbent for removal of two cationic dyes, malachite green (MG) and crystal violet (CV), from aqueous solution. In batch experiments, the effects of contact time, particle size, absorbent dose, solution pH, initial dye concentration, and temperature of MG and CV ions on the pumice adsorption capacity was studied. The characterization of the pumice has been accomplished by X-ray fluorescence spectroscopy, scanning electron microscope, and Brunauer–Emmett–Teller technologies. Equilibrium data were accurately fitted onto Langmuir, Freundlich, and Temkin isotherms. The results showed that the adsorption isotherm data were fitted well to the Langmuir isotherm and the maximum adsorption capacities calculated were 22.57 and 6.99 mg/g for MG and CV at 25°C, respectively. The kinetic data for both dyes were better described by the pseudo-second-order kinetic model. The thermodynamic parameters such as ΔG°, ΔH°, and ΔS° were also evaluated. The positive ΔH° and ΔS° values described endothermic nature of the adsorption and the affinity of pumice for MG and CV adsorption, respectively. It is expected that pumice can be considered as a low-cost adsorbent for the removal of dyes from wastewater.

Keywords: Pumice; Malachite green; Crystal violet; Adsorption; Kinetics; Thermodynamics

1. Introduction

Dye removal from industrial effluents, such as textiles, leather, paper-making industries, plastics, printing, pharmaceutical, electroplating, jute, wool, dyestuff manufacturing, cosmetics and pharmaceuticals, has become a significant issue in recent years [1–4]. Among these dyes, MG and CV cationic dyes are carcinogenic, genotoxic, mutagenic, and teratogenic compared to anionic dye due to their synthetic origin and aromatic ring structure with delocalized electrons [5,6]. As most of these organic dyes in industrial effluents are damaging living aquatic organisms, therefore, it is very necessary to remove dyes from industrial effluents before it is discarded into the aquatic environment [7].

Till now, the methods for the removal of ions and dyes from wastewater are adsorption [8–11], ion

---

*Corresponding author.

exchange [12,13], precipitation [14], electrochemical oxidation [15,16], ultrafiltration [17], adsorption–photocatalytic degradation, etc. [18]. Among these techniques, adsorption is more promising than other available water treatment techniques for the removal of dyes from aqueous solutions, due to its flexible, more convenient, sample of design, clean, effective, and economical method [19–22].

Therefore, several low-cost adsorbents have been used for dye treatment such as hen feather [20,23], coniferous pinus bark powder [3], bottom ash [24,25], red mud [26], ginger waste [6,27], bentonite [28], *Hibiscus cannabinus* fiber [29], vitreous tuff mineral [30], sawdust [31], and leaf powders [19,32].

Geomaterials such as bentonite, pumice, and montmorillonite are natural adsorbent that exhibit good adsorption capacity in the treatment of wastewater [28,33,34]. Generally, pumice is a light stone and ranging from cream, blue, or gray, to green-brown or black. Pumice is a porous and crystal structure volcanic rock produced by the release of gasses during solidified volcanic lava. Volcanic pumice has a large surface area and skeleton structure with highly microvesicular glass pyroclastic which contains open channels that allow ions to travel into the structure [33,35–37]. In addition, this material is available in many countries such as Iran [33], Turkey [38], Ethiopia [39], and Italy [40].

In this study, the capabilities of pumice powder as an adsorbent were tested for the removal of two cationic dyes, malachite green (MG) and crystal violet (CV) from aqueous solution. A series of experiments such as effects of contact time, pH, initial dye concentration, particle size, adsorbent dose, and temperature on the adsorption were investigated. The kinetics, isotherms of dyes, and thermodynamic studies were also performed.

2. Materials and methods

2.1. Chemicals

CV and MG used in this work were obtained from Merck (Merck Co., Germany) and used without

Table 1
The physical and chemical characteristics of CV and MG

Dye	Molecular weight (g/mol)	λ_{max} (nm)	Molecular structure
Crystal violet	407.99	590	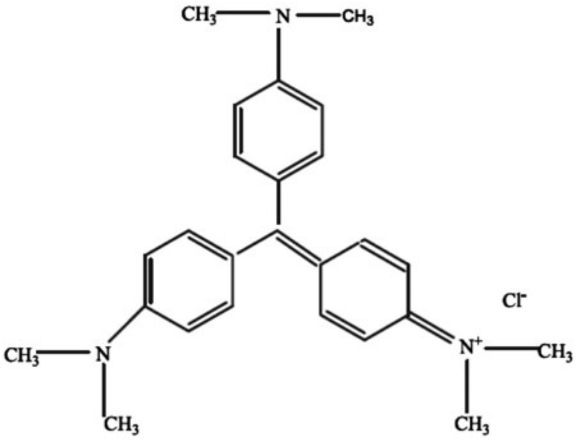
Malachite green	364.92	617	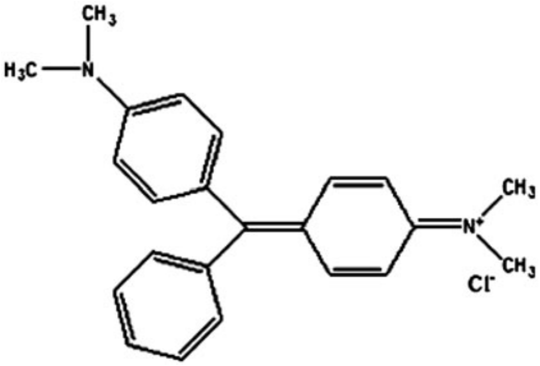

purification. The pH was adjusted and controlled by adding 1 N HCl (Merck) or 1 N NaOH (98%, Merck). The pumice stone used in this study was provided by Alborz Pumice Company (Tehran, Iran). The characteristics and chemical structure of MG and CV dyes are shown in Table 1.

2.2. Preparation of the adsorbent

At first, pumice stone was washed several times with deionized water to remove the primary impurities from their surfaces and dried in a hot air oven at 80℃ for 12 h. Then, the pumice was crushed using ball mill and sieved into four mesh size fractions: mesh size 20–50 (841–297 μm), mesh size 50–100 (297–149 μm), mesh size 100–140 (149–105 μm), and mesh size 140–200 (105–74 μm). Next again, pumice powders washed with deionized water and dried at 80℃ for 24 h. The prepared adsorbent was kept in a plastic container at room temperature for use in adsorption studies.

2.3. Characterization of pumice

The adsorbent morphology was investigated by VEGA\TESCAN scanning electron microscope operated at 30 kV accelerated voltage. The chemical compositions of pumice sample were determined by X-ray fluorescence spectroscopy (XRF) instrument (Philips, Netherlands). Besides, the specific surface area, average pore diameter, and total pore volume were measured on a NOVA® Station B Surface Area Analyzer using the Brunauer–Emmett–Teller (BET) method.

2.4. Batch experiments

To evaluate the adsorption behaviors of MG and CV using the pumice from aqueous solution, batch experiments were conducted. Adsorption experiments were carried out to investigate the effect of contact time (0–150 min), adsorbent dose (5–30 g/L), particle size (mesh size 20–200), pH (2.5–6.5), initial dyes concentration (10–100 mg/L), and temperature (25–65℃), respectively. In each experimental run except for adsorbent dose and particle size, 0.5 g of pumice in mesh size 20–50 was added to 250 mL Erlenmeyer flasks containing 50 mL of 100 mg/L dyes solution and the pH was adjusted (PL-250, EZODO) using 0.5 M NaOH or 0.5 M HCl. The resulting solution was shaken at 125 rpm (cooling incubator-CIT53, Teb Azma, Iran) at constant temperature. After being shaken, the dispersions were centrifuged (EBA-20, HETTICH) for 10 min at 6,000 rpm. The residual concentrations of dyes in the supernatants were analyzed by measuring the dye concentration at λ_{max} using a double beam UV–visible spectrophotometer (Shimadzu UV-1800). Each adsorption sample was carried out twice to avoid any discrepancy between experimental results. The details of the experimental conditions are shown in Table 2.

3. Results and discussion

3.1. Characterization

The main chemical compounds in the pumice stone were silica oxide (SiO_2) and alumina oxide (Al_2O_3). However, the percentage of each compound was different [41,42]. XRF results of volcanic pumice are shown in Table 3.

Table 2
Experimental conditions for dyes adsorption onto the pumice

Experiments	pH	Dye concentration (mg/L)	Adsorbent dose (g/L)	Mesh size	Contact time (min)		Temperature (℃)
					CV	MG	
Effect of contact time	4 ± 0.1 (natural)	100	10	20–50	0–120	0–150	25
Effect of adsorbent dose	4 ± 0.1 (natural)	100	5–30	20–50	120	150	25
Effect of particle size	4 ± 0.1 (natural)	100	10	20–200	120	150	25
Effect of solution pH	2.5–6.5	100	10	20–50	120	150	25
Effect of initial dye concentration	6.5	10–100	10	20–50	120	150	25
Effect of temperature	6.5	100	10	20–50	120	150	25–65

Table 3
Chemical composition of the pumice

Component	% (w/w)	Component	% (w/w)
SiO_2	78.95	MgO	0.77
Al_2O_3	10.87	P_2O_5	0.49
K_2O	2.86	SO_3	0.23
Fe_2O_3	2.39	TiO_2	0.52
CaO	2.92		

Fig. 1(a) shows the SEM micrographs of the pumice sample before and after adsorption of MG and CV dyes. As observed, pumice has an irregular texture and porous surface, which provides suitable sites for adsorption of dye molecule. After adsorption of dyes, large area of the pumice covered with dye molecules which can be seen in Fig. 1(b) and (c).

The surface area and total pore volume of the pumice are calculated by the standard BET method and Horvath–Kawazoe (HK) method. The average pore diameter, surface area, and total pore volume were 24.09 nm, 7.06 m^2/g, and 4.25×10^{-2} cm^3/g, respectively.

3.2. Effect of contact time

The effect of the contact time on the dye adsorption process using the pumice was shown in Fig. 2. As observed, the optimum time for the adsorption of MG and CV was observed as 150 and 120 min, respectively. The adsorption process for MG and CV are described as a two-stage behavior, rapid initial adsorption, and slow rate. Similar results have been reported for the removal of MG by peat of Brunei Darussalam IV [2] and CV onto activated carbon prepared from *Ferula orientalis* [7]. It is clear that rapid adsorption at the initial contact time indicated high affinity between the CV and MG molecules and the pumice surface. As well, the initial contact time can be attributed to the large number of adsorbent sites and high gradient of solute concentration. On the other hand, slow adsorption rate at the end of the experiment can be due to the saturation of the available adsorbing sites and decreased number of vacant sites of adsorbent [19,26].

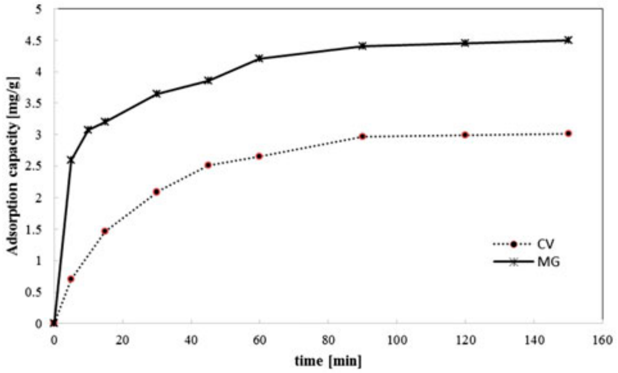

Fig. 2. Effect of contact time on CV and MG adsorption.

3.3. Effect of adsorbent dose

The effect of adsorbent mass is another important factor. According to Fig. 3, removal efficiency increased with increase in adsorbent dose. For CV and MG, removal efficiency increased from 29.90 to 86.68% and 31.62 to 74.84% when the adsorbent dose was increased from 5 to 30 g/L, respectively (Fig. 3(a) and (b)). The enhancement of dye adsorption due to the greater availability of volume active binding sites and an increase in surface area for adsorption [33,43]. On the other hand, for CV and MG the adsorption capacity decreased from 5.98 to 2.88 mg/g and 6.32 to 2.94 mg/g with increased adsorbent dose, respectively (Fig. 3(a) and (b)). The decrease in adsorption capacity

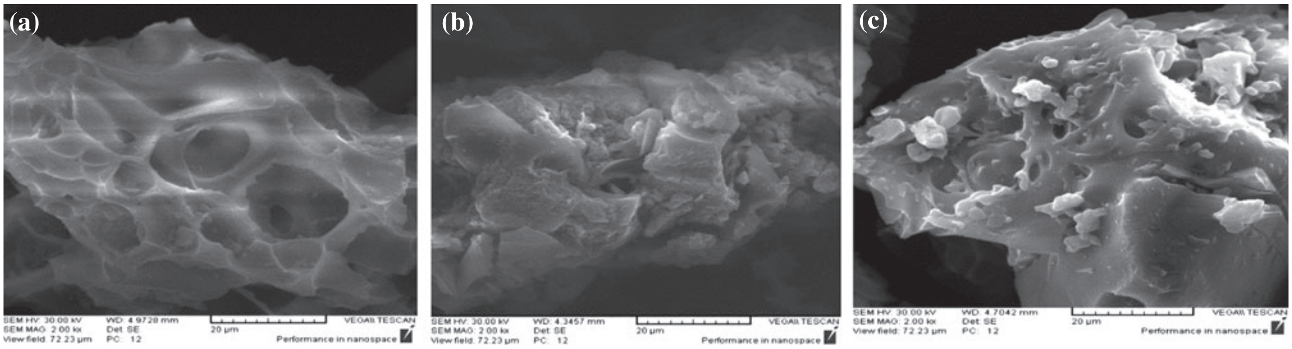

Fig. 1. SEM micrographs of the pumice adsorbent (a), after MG (b), and CV (c) adsorption.

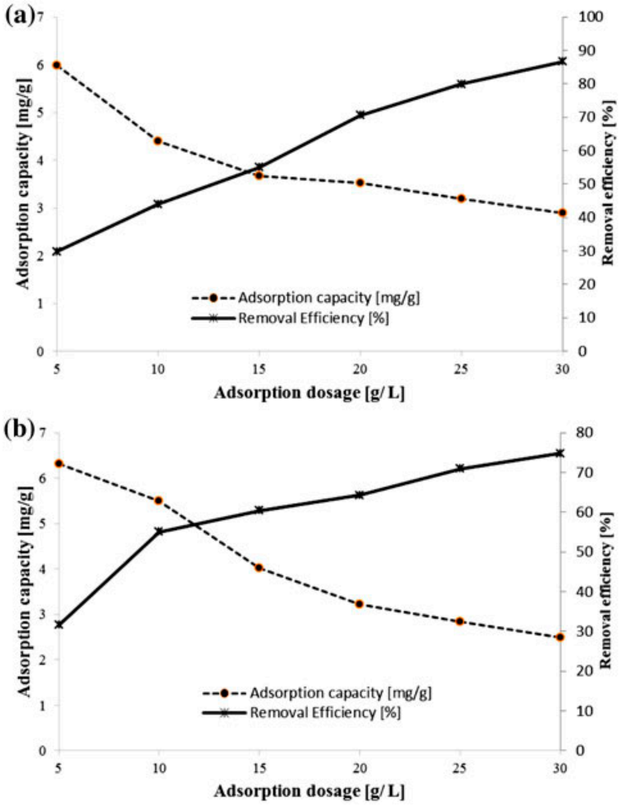

Fig. 3. Effect of adsorbent dose on CV (a) and MG (b) adsorption.

values of pumice is mainly due to the sites remaining unsaturated during the adsorption process and excess amount of adsorbent required for the sorption of dyes [32,33].

3.4. Effect of particle size

The surface area available is an important controlling parameter in the adsorption process. Removal efficiency increased with decrease in the particle size. This relatively between particle size and removal efficiency can be attributed larger total surface area that is associated with smaller particles [44].

For dyes adsorbed onto the pumice, the effect of particle size on removal efficiency is not as such important. For CV and MG, removal efficiency increased from 29.90 to 32.44% and 45.34 to 47.55% when the particle size increased from mesh size 20 to 200, respectively (figure not shown). This result indicated that the pore space of pumice is a continuum and pumice has skeletal structure. Similar results have been reported for the removal of cadmium [41] and nickel [39] by pumice samples.

3.5. Effect of solution pH

The pH of the solution is an important parameter that controls the surface charge of the adsorbent [45]. Experiments were carried out with pH values up to 6.5 due to the fact that dye colorless occurred at alkaline conditions [17,46]. These reactions have been shown in Fig. 4. The adsorption capacity of the pumice vs. pH is given in Fig. 5. Maximum adsorption for both dyes was observed at pH 6.5. For both dyes, CV and MG, the uptake increased with increasing pH, and it increased from 2.06 to 4.43 and 3.85 to 7.53 mg/g for the increase in pH from 2.5 to 6.5, respectively. This would indicate that the adsorption mechanism for both dyes might be similar at this condition. Similar results have been reported for the removal of MG by melamine/maleic anhydride [47] and CV onto activated sintering process red mud [26].

Dyes give positively charged ions when dissolved in water. On the other hand, raw pumice has a negative charge in the entire pH range [37]. Thus, in acidic mediums ($\text{pH} < 7$), a negatively charged surface site on the adsorbent favors the adsorption of cationic dye due to the electrostatic attraction [48].

3.6. Adsorption isotherms

The pumice adsorption capacity with different dye concentrations at equilibrium are shown in Fig. 6. According to Fig. 6, the dye adsorption capacities increased from 0.43 to 7.53 mg/g for MG and from 0.91 to 5.56 mg/g for CV. Generally, for both dyes, the adsorption capacity increased with the increasing dye equilibrium concentration. A higher initial concentration could increase the driving force to overcome the mass transfer resistance and enhance the probability of collision between the dye molecules and the pumice. But, compared to MG, CV is reached to the saturation plateau. It was also found that pumice have lower unsaturated binding sites during the adsorption process of CV [26].

The adsorption parameters were evaluated using Langmuir, Freundlich, and Temkin isotherm models [7,12,33]. The calculated values of these isotherms are given in Table 4. As observed, the value of R^2 obtained from Langmuir, was 0.9994 and 0.9951 for MG and CV, respectively. This fact indicated that Langmuir isotherm model, compared to Freundlich and Temkin isotherm models, could well describe the dyes adsorption on pumice.

3.7. Adsorption kinetics

In order to describe the adsorption kinetics for the adsorption the pseudo-first-order, pseudo-second-order,

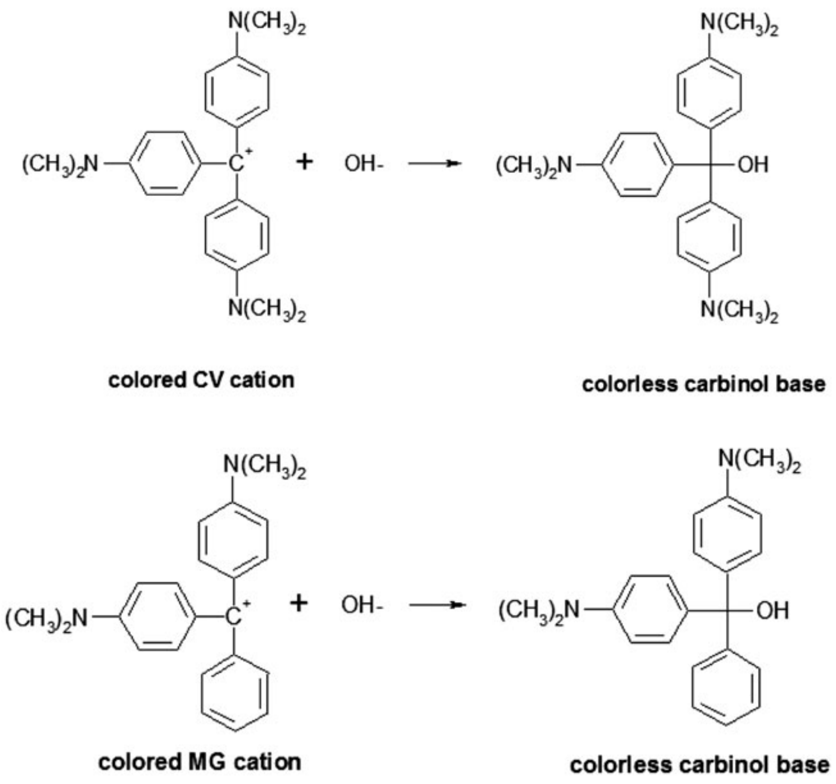

Fig. 4. Reaction of CV and MG with the hydroxide ion.

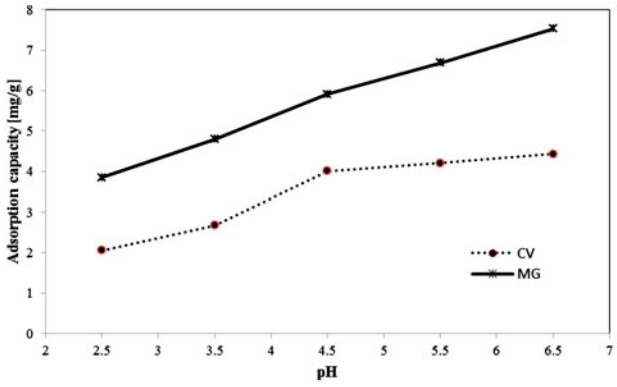

Fig. 5. Effect of pH on CV and MG adsorption.

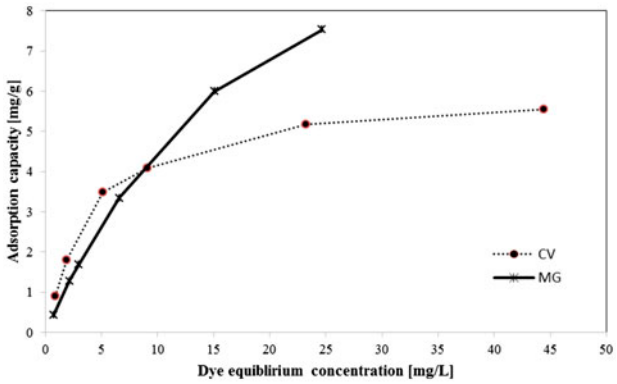

Fig. 6. Isotherms of dyes for adsorption of MG and CV onto the pumice.

and intra-particle diffusion models were applied to test the experimental data which are shown in linear form by the following equations, respectively [7,26].

$$\log(q_\mathrm{e} - q_t) = \log q_\mathrm{e} - \frac{k_1}{2.303}t \tag{1}$$

$$\frac{t}{q_t} = \frac{1}{k_2 q_\mathrm{e}^2} + \frac{t}{q_\mathrm{e}} \tag{2}$$

$$q_t = k_\mathrm{id} t^{1/2} + C \tag{3}$$

According to Eqs. (1)–(3), the plots of log (q_e–q_t) vs. t, t/q_t vs. t and q_e vs. $t^{1/2}$ should each produce a straight line (Fig. 7). The values of correlation coefficient (R^2) obtained from pseudo-second-order kinetics, 0.9989 and 0.9984 for MG and CV, respectively, were higher than those from pseudo-first-order

Table 4
Adsorption isotherm constants for adsorption of dyes onto the pumice

	Langmuir				Freundlich			Temkin		
	q_m (mg /g)	K_L (L/mg)	R^2	R_L	K_F (mg/g) (L/mg)$^{1/n}$	$1/n$	R^2	b_T (J/mol)	K_T (L/g)	R^2
MG	22.57	0.0266	0.9994	0.27–0.88	0.6377	0.8167	0.988	1,162.588	1.0535	0.9323
CV	6.99	0.1699	0.9951	0.06–0.37	1.2662	0.4515	0.9	1,970.7683	2.5914	0.9844

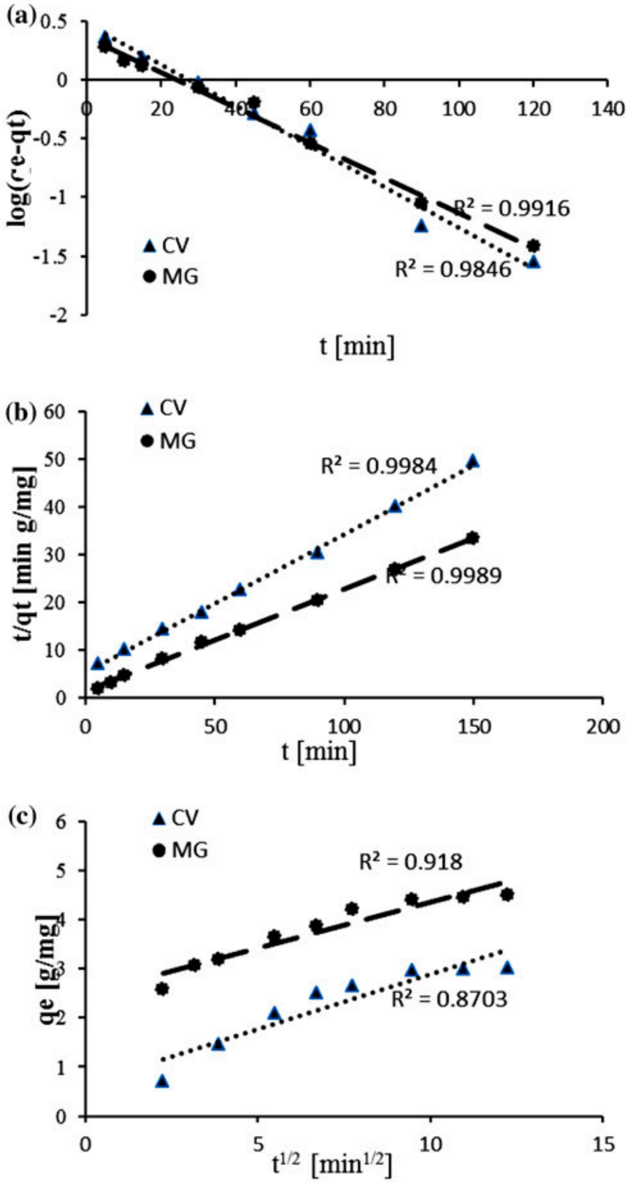

Fig. 7. Adsorption kinetics of MG and CV adsorbed by pumice: (a) pseudo-first-order model, (b) pseudo-second-order model, and (c) intra-particle diffusion model.

kinetics and intra-particle diffusion model. In addition, for both dyes, the experimental q_e values (4.50 mg/g for MG and 3.02 mg/g for CV) were closer to the obtained values from the pseudo-second-order kinetic model (4.68 mg/g for MG and 3.45 mg/g for CV), and thus this model could reasonably describe the MG and CV adsorption on the pumice.

3.8. Adsorption thermodynamic

The change in standard free energy ΔG° (J/mol) evaluated using the following equations [33]:

$$K_D = \frac{qe}{Ce} \tag{4}$$

$$\Delta G^\circ = -RT \ln K_D \tag{5}$$

Then, the change in enthalpy ΔH° (J/mol) and entropy ΔS° (J/(mol K)) were calculated from the following equations (van't Hoff):

$$\ln K_D = \frac{\Delta S^\circ}{R} - \frac{\Delta H^\circ}{RT} \tag{6}$$

The plots of ln K_D against $1/T$ produced a straight line (Fig. 8), from which the values of ΔH° and ΔS° were calculated from the slope and intercept and value of ΔG° was evaluated using Eq. (5). The calculated thermodynamic parameters for both MG and CV are listed in Table 5. The positive value of ΔH° and ΔS° for both dyes indicating that the adsorption process is

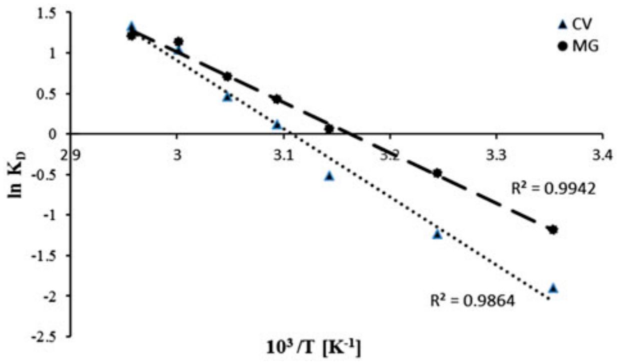

Fig. 8. van't Hoff plot for the adsorption of MG and CV onto the pumice.

Table 5
Adsorption thermodynamic parameters for adsorption of dyes onto the pumice

	ΔH° (J mol^{-1})	ΔS° (J mol^{-1} K^{-1})	ΔG° (J mol^{-1})						
			298	308	318	323	328	333	338
MG	51.79	163.82	2,940.14	1,242.44	−171.38	−1138.40	−1,922.1	−3,145.77	−3,405.99
CV	69.93	217.32	4,718.36	3,185.44	1,385.72	−292.03	−1,238.54	−2,867.61	−3,733.21

endothermic and randomness, respectively. Further, the negative values of ΔG° at many experimental temperatures indicate that the adsorption of MG and CV on the pumice is thermodynamically favorable. On the other hand, at the lowest experimental temperature of 25–35℃ for MG and 25–45℃ for CV, positive ΔG° indicates that the sorption process is less favorable at this temperature, as compared to that at higher temperatures. Similar results have been reported for the removal of methylene blue and MG dyes from aqueous solution by peat of Brunei Darussalam IV [2].

4. Conclusion

In this study, the adsorption characteristics and mechanisms of MG and CV onto the pumice were investigated. For both dyes, the operating parameters for the maximum adsorption were temperature of 298 K, contact time of 150 min, pH of 6.5, adsorbent dosage of 0.5 g and initial dye concentration of 100 mg/L. The adsorption behavior was better described by the Langmuir isotherm model than the Freundlich and Temkin isotherm model, and the calculated adsorption capacities were 22.57 and 6.99 mg/g for MG and CV, respectively. The kinetics of MG and CV adsorption on the pumice were followed the pseudo-second-order rate model. The positive ΔH° and ΔS° values described endothermic nature of the adsorption and the affinity of pumice for MG and CV adsorption, respectively. These results indicate that pumice would be used as an alternative material for the removal of MG and CV dyes and it is expected that pumice can be considered as a low-cost adsorbent for the removal of dyes from wastewater.

References

[1] Y. Zhou, M. Zhang, X. Wang, Q. Huang, Y. Min, T. Ma, J. Niu, Removal of crystal violet by a novel cellulose-based adsorbent: Comparison with native cellulose, Ind. Eng. Chem. Res. 53 (2014) 5498–5506.

[2] H. Chieng, T. Zehra, L.L. Lim, N. Priyantha, D.T.B. Tennakoon, Sorption characteristics of peat of Brunei Darussalam IV: Equilibrium, thermodynamics and kinetics of adsorption of methylene blue and malachite green dyes from aqueous solution, Environ. Earth Sci. 72 (2014) 2263–2277.

[3] R. Ahmad, Studies on adsorption of crystal violet dye from aqueous solution onto coniferous pinus bark powder (CPBP), J. Hazard. Mater. 171 (2009) 767–773.

[4] R. Ahmad, P.K. Mondal, Application of modified water nut carbon as a sorbent in congo red and malachite green dye contaminated wastewater remediation, Sep. Sci. Technol. 45 (2010) 394–403.

[5] A. Appusamy, I. John, K. Ponnusamy, A. Ramalingam, Removal of crystal violet dye from aqueous solution using triton X-114 surfactant via cloud point extraction, Eng. Sci. Technol. Int. J. 17 (2014) 137–144.

[6] R. Ahmad, R. Kumar, Adsorption studies of hazardous malachite green onto treated ginger waste, J. Environ. Manage. 91 (2010) 1032–1038.

[7] T. Aysu, M.M. Küçük, Removal of crystal violet and methylene blue from aqueous solutions by activated carbon prepared from *Ferula orientalis*, Int. J. Environ. Sci. Technol. (in press) 1–12. Available from <http://link.springer.com/article/10.1007%2Fs13762-014-0623-y>.

[8] E. Bulut, M. Özacar, İ.A. Şengil, Adsorption of malachite green onto bentonite: Equilibrium and kinetic studies and process design, Microporous Mesoporous Mater. 115 (2008) 234–246.

[9] M. Toor, B. Jin, S. Dai, V. Vimonses, Activating natural bentonite as a cost-effective adsorbent for removal of Congo-red in wastewater, J. Ind. Eng. Chem. 21 (2015) 653–661.

[10] X. Guo, Q. Wei, B. Du, Y. Zhang, X. Xin, L. Yan, H. Yu, Removal of basic dyes (malachite green) from aqueous medium by adsorption onto amino functionalized graphenes in batch mode, Desalin. Water Treat. 53 (2013) 818–825.

[11] T. Zehra, N. Priyantha, L.B.L. Lim, E. Iqbal, Sorption characteristics of peat of Brunei Darussalam V: Removal of Congo red dye from aqueous solution by peat, Desalin. Water Treat. 54 (2014) 2592–2600.

[12] A. Saeed, M. Sharif, M. Iqbal, Application potential of grapefruit peel as dye sorbent: Kinetics, equilibrium and mechanism of crystal violet adsorption, J. Hazard. Mater. 179 (2010) 564–572.

[13] M. Naushad, A. Mittal, M. Rathore, V. Gupta, Ion-exchange kinetic studies for Cd(II), Co(II), Cu(II), and Pb(II) metal ions over a composite cation exchanger, Desalin. Water Treat. 54 (2014) 2883–2890.

[14] Y.-C. Lee, E.J. Kim, J.-W. Yang, H.-J. Shin, Removal of malachite green by adsorption and precipitation using aminopropyl functionalized magnesium phyllosilicate, J. Hazard. Mater. 192 (2011) 62–70.

[15] S. Raghu, C.W. Lee, S. Chellammal, S. Palanichamy, C.A. Basha, Evaluation of electrochemical oxidation techniques for degradation of dye effluents—A

comparative approach, J. Hazard. Mater. 171 (2009) 748–754.

[16] R.N. Goyal, A. Kumar, A. Mittal, Oxidation chemistry of adenine and hydroxyadenines at pyrolytic graphite electrodes, J. Chem. Soc. Perkin Trans. 2 (1991) 1369–1375.

[17] H. Ouni, M. Dhahbi, Spectrometric study of crystal violet in presence of polyacrylic acid and polyethylenimine and its removal by polyelectrolyte enhanced ultrafiltration, Sep. Purif. Technol. 72 (2010) 340–346.

[18] A. Pourjavadi, S.H. Hosseini, F. Seidi, R. Soleyman, Magnetic removal of crystal violet from aqueous solutions using polysaccharide-based magnetic nanocomposite hydrogels, Polym. Int. 62 (2013) 1038–1044.

[19] M. Peydayesh, A. Rahbar-Kelishami, Adsorption of methylene blue onto *Platanus orientalis* leaf powder: Kinetic, equilibrium and thermodynamic studies, J. Ind. Eng. Chem. 21 (2015) 1014–1019.

[20] J. Mittal, V. Thakur, A. Mittal, Batch removal of hazardous azo dye Bismark Brown R using waste material hen feather, Ecol. Eng. 60 (2013) 249–253.

[21] H. Daraei, A. Mittal, M. Noorisepehr, J. Mittal, Separation of chromium from water samples using egg shell powder as a low-cost sorbent: Kinetic and thermodynamic studies, Desalin. Water Treat. 53 (2013) 214–220.

[22] H. Daraei, A. Mittal, J. Mittal, H. Kamali, Optimization of Cr(VI) removal onto biosorbent eggshell membrane: Experimental & theoretical approaches, Desalin. Water Treat. 52 (2014) 1307–1315.

[23] A. Mittal, J. Mittal, Hen Feather: A Remarkable Adsorbent for Dye Removal, Green Chemistry for Dyes Removal from Wastewater: Research Trends and Applications, John Wiley & Sons, Hoboken, NJ, 2015, pp. 409–457.

[24] A. Mittal, L. Kurup, Column operations for the removal & recovery of a hazardous dye 'Acid Red—27' from aqueous solutions, using waste materials—Bottom ash and de-oiled soya, ecology, Environ. Conserv. 13 (2006) 181–186.

[25] J. Mittal, D. Jhare, H. Vardhan, A. Mittal, Utilization of bottom ash as a low-cost sorbent for the removal and recovery of a toxic halogen containing dye eosin yellow, Desalin. Water Treat. 52 (2014) 4508–4519.

[26] L. Zhang, H. Zhang, W. Guo, Y. Tian, Removal of malachite green and crystal violet cationic dyes from aqueous solution using activated sintering process red mud, Appl. Clay Sci. 93–94 (2014) 85–93.

[27] R. Kumar, R. Ahmad, Biosorption of hazardous crystal violet dye from aqueous solution onto treated ginger waste (TGW), Desalination 265 (2011) 112–118.

[28] A.A. Oladipo, M. Gazi, Enhanced removal of crystal violet by low cost alginate/acid activated bentonite composite beads: Optimization and modelling using non-linear regression technique, J. Water Process Eng. 2 (2014) 43–52.

[29] G. Sharma, M. Naushad, D. Pathania, A. Mittal, G. El-desoky, Modification of *Hibiscus cannabinus* fiber by graft copolymerization: Application for dye removal, Desalin. Water Treat. 54 (2014) 3114–3121.

[30] A. Blanco-Flores, A. Colín-Cruz, E. Gutiérrez-Segura, V. Sánchez-Mendieta, D.A. Solís-Casados, M.A. Garrudo-Guirado, R. Batista-González, Efficient removal of crystal violet dye from aqueous solutions by vitreous tuff mineral, Environ. Technol. 35 (2014) 1508–1519.

[31] S.D. Khattri, M.K. Singh, Removal of malachite green from dye wastewater using neem sawdust by adsorption, J. Hazard. Mater. 167 (2009) 1089–1094.

[32] S. Neupane, S.T. Ramesh, R. Gandhimathi, P.V. Nidheesh, Pineapple leaf (*Ananas comosus*) powder as a biosorbent for the removal of crystal violet from aqueous solution, Desalin. Water Treat. 52 (2014) 2041–2054.

[33] M.N. Sepehr, A. Amrane, K.A. Karimaian, M. Zarrabi, H.R. Ghaffari, Potential of waste pumice and surface modified pumice for hexavalent chromium removal: Characterization, equilibrium, thermodynamic and kinetic study, J. Taiwan Inst. Chem. E. 45 (2014) 635–647.

[34] L. Guz, G. Curutchet, R.M. Torres Sánchez, R. Candal, Adsorption of crystal violet on montmorillonite (or iron modified montmorillonite) followed by degradation through Fenton or photo-Fenton type reactions, J. Environ. Chem. Eng. 2 (2014) 2344–2351.

[35] T. Liu, Z.-L. Wang, X. Yan, B. Zhang, Removal of mercury(II) and chromium(VI) from wastewater using a new and effective composite: Pumice-supported nanoscale zero-valent iron, Chem. Eng. J. 245 (2014) 34–40.

[36] T. Şahan, D. Öztürk, Investigation of Pb(II) adsorption onto pumice samples: Application of optimization method based on fractional factorial design and response surface methodology, Clean Technol. Environ. Policy 16 (2014) 819–831.

[37] G. Asgari, B. Roshani, G. Ghanizadeh, The investigation of kinetic and isotherm of fluoride adsorption onto functionalize pumice stone, J. Hazard. Mater. 217–218 (2012) 123–132.

[38] D. Turan, C. Kocahakimoğlu, E. Boyacı, S. Sofuoglu, A. Eroğlu, Chitosan-immobilized pumice for the removal of As(V) from waters, Water Air Soil Pollut. 225 (2014) 1–12.

[39] E. Alemayehu, B. Lennartz, Adsorptive removal of nickel from water using volcanic rocks, Appl. Geochem. 25 (2010) 1596–1602.

[40] M. Rosaria Panuccio, F. Crea, A. Sorgonà, G. Cacco, Adsorption of nutrients and cadmium by different minerals: Experimental studies and modelling, J. Environ. Manage. 88 (2008) 890–898.

[41] E. Alemayehu, B. Lennartz, Virgin volcanic rocks: Kinetics and equilibrium studies for the adsorption of cadmium from water, J. Hazard. Mater. 169 (2009) 395–401.

[42] M. Yavuz, F. Gode, E. Pehlivan, S. Ozmert, Y.C. Sharma, An economic removal of Cu^{2+} and Cr^{3+} on the new adsorbents: Pumice and polyacrylonitrile/pumice composite, Chem. Eng. J. 137 (2008) 453–461.

[43] A. Salifu, B. Petrusevski, K. Ghebremichael, L. Modestus, R. Buamah, C. Aubry, G.L. Amy, Aluminum (hydr)oxide coated pumice for fluoride removal from drinking water: Synthesis, equilibrium, kinetics and mechanism, Chem. Eng. J. 228 (2013) 63–74.

[44] W.C. Wanyonyi, J.M. Onyari, P.M. Shiundu, Adsorption of congo red dye from aqueous solutions using roots of *Eichhornia Crassipes*: Kinetic and equilibrium studies, Energy Procedia 50 (2014) 862–869.

[45] B. Heibati, S. Rodriguez-Couto, A. Amrane, M. Rafatullah, A. Hawari, M.A. Al-Ghouti, Uptake of Reactive Black 5 by pumice and walnut activated carbon: Chemistry and adsorption mechanisms, J. Ind. Eng. Chem. 20 (2014) 2939–2947.

[46] Q. Zhang, T. Zhang, T. He, L. Chen, Removal of crystal violet by clay/PNIPAm nanocomposite hydrogels with various clay contents, Appl. Clay Sci. 90 (2014) 1–5.

[47] X. Rong, F. Qiu, J. Qin, J. Yan, H. Zhao, D. Yang, Removal of malachite green from the contaminated water using a water-soluble melamine/maleic anhydride sorbent, J. Ind. Eng. Chem. 20 (2014) 3808–3814.

[48] A. Soni, A. Tiwari, A.K. Bajpai, Removal of malachite green from aqueous solution using nano-iron oxide-loaded alginate microspheres: Batch and column studies, Res. Chem. Intermed. 40 (2014) 913–930.